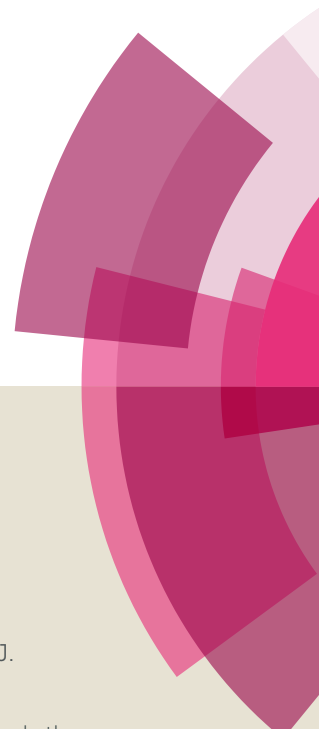


NJC

Accepted Manuscript



This article can be cited before page numbers have been issued, to do this please use: H. Yu, J. Yang, J. Han, P. Li, Y. Hou, W. Wang and M. Fang, *New J. Chem.*, 2019, DOI: 10.1039/C8NJ05109G.



This is an Accepted Manuscript, which has been through the Royal Society of Chemistry peer review process and has been accepted for publication.

Accepted Manuscripts are published online shortly after acceptance, before technical editing, formatting and proof reading. Using this free service, authors can make their results available to the community, in citable form, before we publish the edited article. We will replace this Accepted Manuscript with the edited and formatted Advance Article as soon as it is available.

You can find more information about Accepted Manuscripts in the [author guidelines](#).

Please note that technical editing may introduce minor changes to the text and/or graphics, which may alter content. The journal's standard [Terms & Conditions](#) and the ethical guidelines, outlined in our [author and reviewer resource centre](#), still apply. In no event shall the Royal Society of Chemistry be held responsible for any errors or omissions in this Accepted Manuscript or any consequences arising from the use of any information it contains.

Tetranuclear lanthanide complexes showing magnetic refrigeration and single molecule magnet behavior

Hong Yu,^a Jia-Xing Yang,^b Ju-Qing Han,^b Peng-Fei Li,^a Yin-Ling

Hou,^d * Wen-Min Wang,^b * Ming Fang^{a, c,*}

Abstract:

Three tetranuclear lanthanide complexes: $\{[\text{Ln}_4(\text{L})_6(\text{pbd})_4(\mu_3\text{-OH})_2]\cdot 2\text{CH}_3\text{CN}\}$ ($\text{Ln} = \text{Gd}$ (1), Tb (2), Dy (3); $\text{HL} = 5\text{-}(\text{benzylideneamino})\text{quinolin-8-ol}$, $\text{pbd} = 1\text{-phenylbutane-1,3-dione}$) were fabricated and structurally characterized. Compounds 1-3 are isostructural belonging to the triclinic system with space group $P\bar{1}$. The core of the complexes contain a tetranuclear arrangement of Ln^{III} ions which is held together by two pyramidal $\mu_3\text{-OH}^-$ ions and six μ_2 phenol hydroxyl oxygen atoms derived from six L^- ligands. Magnetic studies indicated that 1 exhibits cryogenic magnetic refrigeration property (maximum $-\Delta S_m = 21.41 \text{ J K}^{-1} \text{ kg}^{-1}$, $\Delta H = 7 \text{ T}$ at 2.0 K), whereas compound 3 exhibits slow relaxation of the magnetization with energy barrier ($\Delta E/k_B$) of 81.48 K and $\tau_0 = 6.48 \times 10^{-8} \text{ s}$.

Keyword: Lanthanide, Tetranuclear compounds, Magnetocaloric effect, Single-molecule magnet behaviour

Introduction

During the past two decades, lanthanide (III) polynuclear clusters have attracted

a Department of Chemistry, Hebei Normal University of Science & Technology, Qinhuangdao 066004, Hebei province, P. R.China. E-mail:fangmingchem@163.com

b Department of Chemistry, Taiyuan Normal University, Jinzhong 030619, PR China. E-mail: wangwenmin0506@126.com

c Key Laboratory of Advanced Energy Materials Chemistry (Ministry of Education), College of Chemistry, Nankai University, Tianjin 300071, China

d School of Life and Health Science, Kaili University, Kaili, 556011, China, hyl0506@126.com

† Electronic supplementary information (ESI) available: Selected bond lengths and angles. CCDC 1871768-1871770. For ESI and crystallographic data in CIF or other electronic format see DOI: 10.1039/c000000x/

great interest because of their potential applications in molecular magnetic materials, such as molecular magnetic refrigeration and single-molecule magnets (SMMs).^[2, 3] Molecular magnetic refrigeration exhibiting an enhanced magnetocaloric effect (MCE) are proposed to replace the expensive and increasingly rare He-3 in ultralow temperature refrigeration.^[4] To our knowledge, the magnetocaloric effect (MCE) represents the change of isothermal magnetic entropy (ΔS_m) and adiabatic temperature (ΔT_{ad}) with external magnetic field variation.^[5] In general, an outstanding molecular magnetic refrigeration requires a large spin multiplicity associated with a negligible anisotropy.^[6] Thus, Gd³⁺ is a common constituent element for molecular refrigerant materials, because it is favored by it having a ⁸S_{7/2} ground-state term (S=7/2, L=0), with high spin and zero orbital momentum, and therefore no spin-orbit coupling is possible. These theoretical perspectives were further supported by a large amount of Gd-containing clusters have been reported,^[7] such as, the Gd₁₀₄ with large magnetic entropy change of $\Delta S_m = 46.9 \text{ J kg}^{-1} \text{ K}^{-1}$ (T = 2.0 K and $\Delta H = 7 \text{ T}$)^[6a] and Gd₆₀ with large $\Delta S_m = 66.5 \text{ J kg}^{-1} \text{ K}^{-1}$ (T = 3.0 K and $\Delta H = 7 \text{ T}$).^[8]

Furthermore, since the discovery of Ishikawa et al.'s double-decker compound (Bu₄N)[Tb(Pc)₂] (H₂Pc = phthalocyanine) shows slow relaxation of the magnetization at low temperature,^[9] considerable attentions have been paid toward introducing 4f ions into SMMs in either mixed 3d/4f or pure 4f systems because of their inherent magnetic anisotropy arising from a large, unquenched orbital angular momentum.^[10-13] In particular, dysprosium plays a crucial role because of its unparalleled single-ion anisotropy and the spinparity effect for a Kramers ion, which is responsible for numerous ground-breaking results.^[12,13] Such as, Layfield group reported a dysprosium metallocene with a record energy barrier $U_{eff} = 1837 \text{ K}$ in zero field and a blocking temperature of 60 K,^[12] exceeding the previous one ($U_{eff} = 1815 \text{ K}$) reported by Zheng's group.^[13] These excellent results attracted more and more researcher focus on the study of Ln-SMMs.

The Dy (III) ions are ideal for constructing SMMs with high energy barriers, benefiting from both the high moment and the high anisotropy of the spin-orbit coupled Dy (III) Kramers doublet ground state.^[14] However, the magnetic exchange

effect between Dy (III) ions is weakened by the shielding effect of 5s and 5p orbitals, meanwhile, quantum tunneling phenomenon often occurs in such complexes, resulting in the reduction of effective potential energy barrier. Therefore, how to increase the magnetic exchange between ions and suppress the quantum tunneling effect is the key to improving the energy barrier of Dy-SMMs. The ligand field surrounding lanthanide ions play an important role in tuning the magnetic properties of SMMs, and a slight difference in the structure may have an effect on the directions of easy axes, thus resulting in different slow relaxation behaviors.^[15] In a quest for excellent magnetic behaviors for Ln(III)-based polynuclear species, an attractive 8-hydroxyquinoline Schiff base derivative ligand was employed to construct lanthanide polynuclear compounds, which have excellent structural features: (i) it can easily coordinate with Ln(III) ions through N and O donor atoms; (ii) the phenoxy atom of the ligand can act as a bridge between Ln(III) ions centers, which can transmit magnetic exchange efficiently. Taking advantage of this ligand, three tetranuclear lanthanide complexes with a general formula $\{[\text{Ln}_4(\text{L})_6(\text{pbd})_4(\mu_3\text{-OH})_2]\cdot 2\text{CH}_3\text{CN}\}$ (Ln = Gd (**1**), Tb (**2**), Dy (**3**); HL = 5-(benzylideneamino)quinolin-8-ol, pbd = 1-phenylbutane-1,3-dione) were fabricated and structurally characterized. Magnetic study reveals that **1** exhibits cryogenic magnetic refrigeration property with maximum $-\Delta S_m = 21.41 \text{ J K}^{-1} \text{ kg}^{-1}$ for $\Delta H = 7 \text{ T}$ at 2.0 K, whereas **3** displays slow relaxation of the magnetization ($\Delta E/k_B = 61.6 \text{ K}$ and $\tau_0 = 2.77 \times 10^{-6} \text{ s}$).

Experimental section

Materials and Physical Measurements.

All chemicals purchased were of reagent grade and used without further purification. Water used in the reactions is distilled water. Analyses for C, H and N were carried out on a Perkin-Elmer analyzer. IR spectra were collected in the range of 400–4000 cm^{-1} with a Bruker TENOR 27 spectrophotometer using KBr pellets. ¹H NMR spectrum was performed on a Bruker Avance III HD 500 MHz instrument. PXRD data were examined on a Rigaku Ultima IV instrument with Cu K α radiation

($\lambda = 1.54056 \text{ \AA}$), with a scan speed of $10^\circ \text{ min}^{-1}$ in the range of $2\theta = 5-50^\circ$. View Article Online
DOI: 10.1039/C8NJ05109G

Luminescence properties were recorded on an F-4500 FL spectrophotometer with a xenon arc lamp as the light source. Magnetic susceptibilities were performed on a Quantum Design MPMS-XL7 and a PPMS-9 ACMS magnetometer. Diamagnetic corrections were made with Pascal's constants for all the constituent atoms.

Crystallographic studies.

Single-crystal X-ray diffraction measurements of **1** - **3** were carried out at room temperature on a CCD X-ray diffractometer equipped with graphite monochromated $\text{MoK}\alpha$ radiation ($\lambda = 0.71073 \text{ \AA}$). Lorentz polarization and absorption corrections were applied. The structure was solved by direct methods and refined with a full-matrix least-squares technique based on F^2 using the SHELXS-97 and SHELXL-97 programs.^[16] All the nonhydrogen atoms were refined with anisotropic parameters while H atoms were placed in calculated positions and refined using a riding model. The disorder of solvent molecules is serious, so squeeze was used to process this data, and molecular formula of **1-3** is determined by elemental analysis. Crystallographic data for **1** – **3** were summarized in Table 1. Selected bond lengths and angles were summarized in Table S1-S3.

Table 1 Crystallographic Data and Structure Refinements for **1-3**

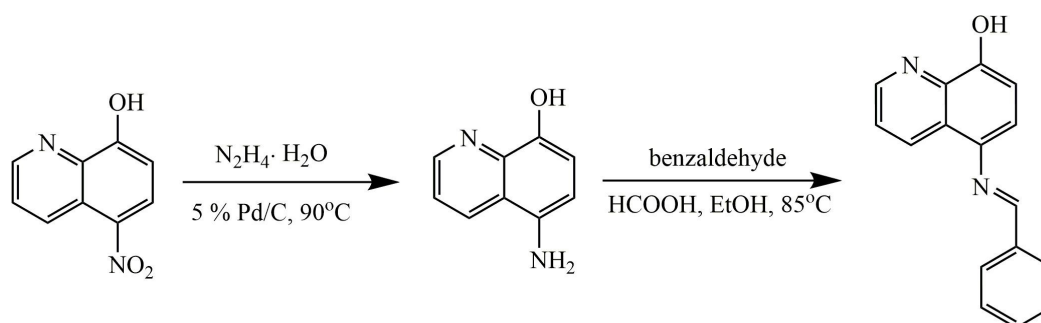
	1	2	3
Formula	$\text{C}_{140}\text{H}_{110}\text{Gd}_4\text{N}_{14}\text{O}_{16}$	$\text{C}_{140}\text{H}_{110}\text{N}_{14}\text{O}_{16}\text{Tb}_4$	$\text{C}_{140}\text{H}_{110}\text{Dy}_4\text{N}_{14}\text{O}_{16}$
<i>Mr</i> (g mol ⁻¹)	2873.41	2880.09	2894.5
Cryst syst	triclinic	triclinic	triclinic
Space group	<i>P</i> -1	<i>P</i> -1	<i>P</i> -1
<i>a</i> (Å)	14.9021(8)	14.9151(7)	13.7157(6)
<i>b</i> (Å)	15.4352(10)	15.4503(8)	16.2542(8)
<i>c</i> (Å)	15.5643(10)	15.5107(8)	17.1198(7)
α (°)	80.276	80.272	87.098
β (°)	67.618	67.467	89.370
γ (°)	68.757	68.699	86.006
<i>V</i> (Å ³)	3083.4(3)	3074.1(3)	3802.4(3)
<i>Z</i>	1	1	1
<i>D_c</i> (g cm ⁻³)	1.547	1.556	1.264
μ (mm ⁻¹)	2.195	2.345	1.998

$\theta/^\circ$	2.448 to 25.010	2.430 to 26.418	2.186 to 25.372
$F(000)$	1432	1436	1396
Reflns collected	35405	50754	56611
Unique reflns	10790	12629	13934
R_{int}	0.0711	0.0988	0.1160
GOF on F^2	1.073	1.010	1.033
$R_1, wR_2 [I > 2\sigma(I)]$	0.0909, 0.2220	0.0478, 0.0870	0.0455, 0.0935
$R_1, wR_2(\text{all date})$	0.1415, 0.2668	0.0938, 0.0982	0.0948, 0.1067

View Article Online
DOI: 10.1039/C8NJ05109G

Synthesis of 5-aminoquinolin-8-ol.

A mixture of 5-nitroquinolin-8-ol (50 mmol) and 5 % Pd/C (0.75 g), which was used as catalyst, in a 1.3 % ratio in absolute isopropanol was heated to 65 °C, and then 12 mL of 85 % hydrazine hydrate was dropped into the mixture over 1 h. It was heated to 90 °C and refluxed for 6 h. Finally, the solvent was removed, and dichloromethane was used to wash the grass green solid product (yield: 50.8%). Elemental analysis (%): Calcd for C₉H₈ON₂ (F_w = 160.42): C 67.32, H 5.00, N 17.50. Found: C 67.28, H 4.97, N 17.82.



Scheme 1. The synthesis of HL.

Synthesis of 5-(benzylideneamino)quinolin-8-ol (HL)

The Schiff base ligand 5-(benzylideneamino)quinolin-8-ol (HL) was synthesized in a simple aldimine condensation reaction of 5-aminoquinolin-8-ol (10 mmol) with benzaldehyde (10 mmol) in 50 mL ethanol with the catalyze of 5 drops formic acid (Scheme 1). The reaction mixture was stirred for 5 h at 85 °C. The product was isolated from the mixture and it was purified by recrystallization from a mixed solvent of ethanol and acetone (3/1, v/v). The purified product was obtained as a green solid (yield 2.0 g, 80.6%). Elemental analysis (%): Calcd for C₁₆H₁₂ON₂ (F_w = 248.28): C

77.40, H 4.87, N 11.28. Found: C 77.28, H 4.97, N 11.22. The IR spectra and ¹H NMR spectrum (500 MHz, CDCl₃) of the ligand are shown in Figure S1 and Figure S2.

Synthesis of Complexes 1–3

The compounds **1–3** were obtained by the reaction of Ln(pbd)₃·2H₂O (0.025 mmol; Ln(III) = Gd (**1**), Tb (**2**), Dy (**3**)) and HL (0.025 mmol) in mixture solution containing 8 mL acetonitrile and 4 mL dichloromethane. The solution was sealed in a 20 mL vial and heated at 70 °C for 24 h, followed by cooling to room temperature slowly. Yellow block shaped crystals suitable for single-crystal X-ray data collection was isolated. Yield: 64%, 62%, and 58% based on HL for **1–3**, respectively. Elemental analysis found (%) for C₁₄₀H₁₁₀Gd₄N₁₄O₁₆ (**1**): C 58.56, H 3.77, N 6.88; for C₁₄₀H₁₁₀N₁₄O₁₆Tb₄ (**2**): C 58.44, H 3.89, N 6.85; for C₁₄₀H₁₁₀Dy₄N₁₄O₁₆ (**3**): C 58.05, H 3.76, N 6.79.

Results and Discussion

Crystal structures of compounds 1 – 3

Single crystal X-ray diffraction analyses reveal that the three compounds are isostructural, and crystallize in the triclinic space group *P*–1 (Table 1), with *Z* = 1. The structure of **3** (Ln = Dy) will be described here as a representative example of the series. The molecular structure (Figure 1) consists of a precisely coplanar [Dy₄] core with crystallographic inversion symmetry (Figure 2), in which two pyramidal μ₃–OH[–] oxygen atoms (O8) are located at the opposite sides of the [Dy₄] plane and are displaced out of that plane by 0.89 Å. The bond distances of Dy–O8 are 2.347(4), 2.340(4) and 2.352(4) Å, and the Dy–O8–Dy angles 110.45(16), 110.82(16) and 98.08(15), and a Dy–Dy distance of 3.8593(6), 3.5434(4) and 3.8582(5) Å. The tetranuclear [Dy₄] ions are further bridged by six μ₂ phenol hydroxyl oxygen atoms (O1, O2, O3) derived from six L[–] ligands, generating a [Dy₄O₈] core. The L[–] ligand serves as a didentate ligand and chelates the central Dy(III) ions through one phenol hydroxyl oxygen atom (O1/O2/O3) and one pyridyl nitrogen (N2/N4/N6), and the oxygen atom bridge to another Dy(III) ions; and each pbd[–] chelates the Dy atom through two oxygen atoms. Thus, Dy1 is eight-coordinated, chelates by one L[–]

ligands and one pbd⁻, and also coordinate with two μ_3 -OH⁻ oxygen atoms and two μ_2 phenol hydroxyl oxygen atoms from the ligands. While Dy2 is chelated by two L⁻ ligands and one pbd⁻, and coordinate with one μ_3 -OH⁻ oxygen atom and one μ_2 phenol hydroxyl oxygen atom. The Dy-O bond lengths are in the range of 2.290(4)–2.421(4) Å; the Dy-N bond lengths are 2.533(5), 2.558(5) and 2.525(5) Å. These values are comparable to those of the already reported lanthanide complexes.^[17] The coordination geometries for Dy(III) ions in an asymmetry unit were performed by continuous-shape measurements (CShM) using SHAPE 2.0 software. The calculated results listed in Table S4 reveal that the centre Dy³⁺ ions possess square antiprism geometries.

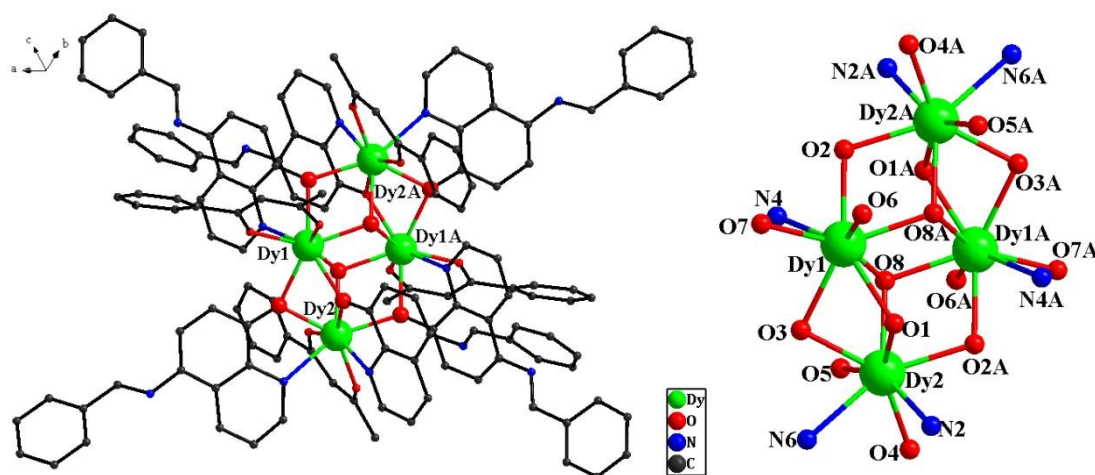


Figure 1. Molecular structure of **3** (left) (all hydrogen atoms are omitted for clarity), the [Dy₄] core bridged by μ_3 -OH⁻ oxygen atom and μ_2 phenol hydroxyl oxygen atom (right).

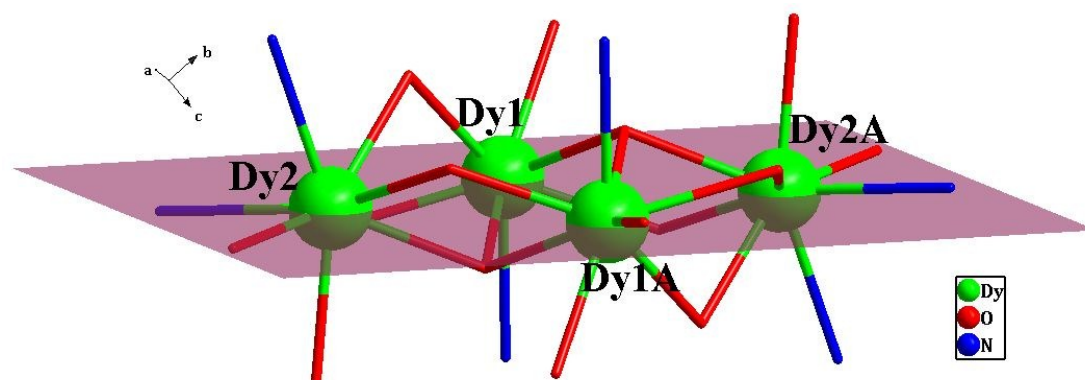


Figure 2. The side view of the [Dy₄O₈] core of **3** (all hydrogen atoms are omitted for clarity).

Powder X-ray diffraction (PXRD)

The purity of crystalline powders of **1-3** were confirmed by powder X-ray

diffraction (PXRD) (Figure S3). The observed PXRD patterns are in good agreement with the results simulated from the single crystal data, suggesting the purity of the solid samples. The differences in intensity could be due to the preferred orientation of the crystalline powder samples.

Luminescence properties of 2

The solid-state luminescence property of **2** was measured at the exciting wavelength of 300 nm at room temperature. As shown in Figure S4, the emission spectrum of **2** exhibits the characteristic emissions of Tb^{III} ion. The emission spectrum presents four peaks at 492, 546, 588 and 621 nm which are assigned to the transition of ⁵D₄ to ⁷F_J (*J* = 6, 5, 4, 3). Among them, the emission peak at 546 nm (⁵D₄→⁷F₅) is the strongest.

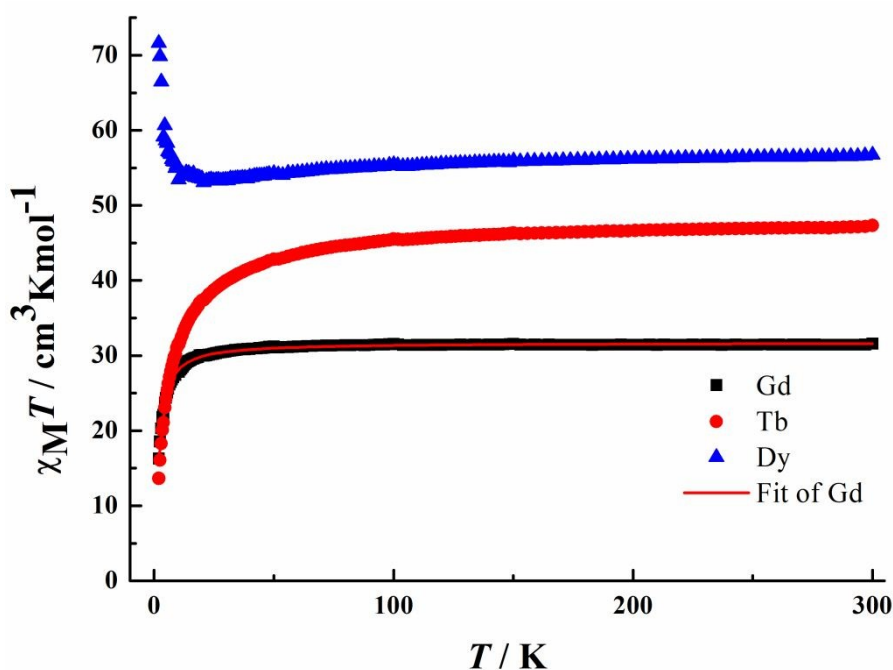


Figure 3. The plots of $\chi_M T$ versus T for **1**(■), **2**(●) and **3**(▲) under 1000 Oe field.

Magnetic Properties of 1-3

The magnetic susceptibility of **1-3** were measured on the microcrystalline samples in the temperature range from 2 to 300 K and under 1000 Oe field, as shown in Figure 3. At room temperature, the $\chi_M T$ value for **1-3** is 31.59, 47.33 and 56.73 cm³ K mol⁻¹ which is close to the corresponding theoretical value of 31.52, 47.28 and 56.68 cm³ K

mol⁻¹ expected for four magnetically Ln³⁺ ions: Gd³⁺ in the ⁸S_{7/2} ground state ($g = 2$) for **1**, Tb³⁺ in the ⁷F₆ ground state ($g = 3/2$) for **2** and Dy³⁺ in the ⁶H_{15/2} ground state ($g = 4/3$) for **3**.^[18] For **1**, the $\chi_M T$ value stays almost constant in the temperature range 300–30 K and then decreases rapidly to a minimum value of 16.27 cm³ K mol⁻¹ at 2 K, which indicates the presence of a weak antiferromagnetic interaction between the adjacent Gd³⁺ ions.^[19] The magnetic interaction was analyzed by means of a dimer law based on the Hamiltonian $\hat{H} = -J\hat{S}_A\hat{S}_B$ with $\hat{S}_A = \hat{S}_B = 7/2$, a corresponding equation as following was deduced, and the magnetic properties of **1** can be appropriately described by it.^[20]

$$\chi_M = 2 * \frac{2Ng^2\beta^2}{kT} \times \frac{e^{J/kT} + 5e^{3J/kT} + 14e^{6J/kT} + 30e^{10J/kT} + 55e^{15J/kT} + 91e^{21J/kT} + 140e^{28J/kT}}{1 + 3e^{J/kT} + 5e^{3J/kT} + 7e^{6J/kT} + 9e^{10J/kT} + 11e^{15J/kT} + 13e^{21J/kT} + 15e^{28J/kT}}$$

Least-squares fitting of the experimental data leads to $J = -0.15$ cm⁻¹, $g = 2.01$, and the agreement factor R , defined as $R = \sum(\chi_{\text{obsd}} - \chi_{\text{calcd}})^2 / \sum(\chi_{\text{obsd}})^2$, is 1.4×10^{-2} . The negative and small J value indicates very weak antiferromagnetic coupling interaction between adjacent Gd³⁺. For lanthanide ions, the 4f electrons are well shielded by outer-shell electrons, compared with 3d electrons, the interaction of 4f electrons from adjacent lanthanide ions is rather weak.

For **2**, as the temperature is lowered, $\chi_M T$ values decreases slightly to 43.54 cm³ K mol⁻¹ at 60 K which may attribute to thermal depopulation of Stark sublevels, with further cooling the $\chi_M T$ values decrease quickly to 13.65 cm³ K mol⁻¹ which may ascribe to antiferromagnetic interactions between adjacent Tb³⁺ ions.^[21] For **3**, the $\chi_M T$ value decreases slowly to 53.57 cm³ K mol⁻¹ on cooling from 300 to 20 K, which may attribute to thermal depopulation of Stark sublevels dominates the magnetic properties above 20 K. With further cooling the $\chi_M T$ values increases quickly to 71.63 cm³ K mol⁻¹ at 2 K. This behavior is indicative of the presence of ferromagnetic interactions between adjacent Dy(III) ions.^[21]

The magnetization data of **1** is carried out at a field of 0–8 T between 2 and 10 K. As shown in Figure 4 (left), the M versus H curves display a gradual increase with the increasing field and saturation values of 28.11 $N\beta$ for **1** at 80 kOe and 2 K, which is extremely close to the theoretical value of 28 $N\beta$ for four individual Gd(III) ($S = 7/2$,

$g = 2$) ions. Magnetic entropy changes ΔS_m of **1** can be calculated from the M versus H data to evaluate the MCE. ΔS_m are calculated by using the Maxwell equation:

$$\Delta S_m(T) = \int [\partial M(T, H)/\partial T] H dH \quad (1)$$

According to eq 1,^[22] the $-\Delta S_m$ values of **1** can be obtained; the plots of $-\Delta S_m$ versus T are shown in Figure 4 (right). For **1**, the maximum value of $-\Delta S_m$ is 21.41 J K⁻¹ kg⁻¹ (calculated as $4R\ln(2S+1)$, expected maximum $-\Delta S_m$ is 24.05 J K⁻¹ kg⁻¹ for a field change $\Delta H = 7$ T at 2.0 K. The difference of $-\Delta S_m$ between the experimental and theoretical values for **1** might be due to the antiferromagnetic interaction in **1**.^[23] The maximum $-\Delta S_m$ of **1** is smaller than the antiferromagnetic {Gd₄} complexes which have been reported:^[24] [Gd₄(μ_3 -OH)₂(L)₂L₁L₂(HOCH₃)₂] \cdot 11H₂O {H₂L = 2,3-bis((E)-(2-hydroxy-3-methoxy benzylidene) amino) maleonitrile, HL₁ = (2-amino-3-((E)-(2-hydroxy-3-methoxy benzylidene)amino)maleonitrile), H₃L₂ = ((1E,3Z,8Z,10E)-1,6,11-tris(2-hydroxy-3-methoxyphenyl)-2,5,7,10-tetraazaundeca-1,3,8,10-tetraene-3,4,8,9-tetracarbonitrile), $-\Delta S_m = 27.2$ J kg⁻¹ K⁻¹ for $\Delta H = 7$ T at 3 K}, [Ln₄L₄(OH)₂](OAc)₂ \cdot 4H₂O {H₂L = butanedihydrazidebridgedbis(3-ethoxysalicylaldehyde), $-\Delta S_m = 24.4$ J kg⁻¹ K⁻¹ for $\Delta H = 7$ T at 3 K}, [Gd₄(CO₃)(L)₄(acac)₂(H₂O)₄] \cdot 2CH₃CN (A) and [Ln₄(CO₃)(L)₄(acac)₂(CH₃OH)₂(H₂O)₂] \cdot CH₃OH \cdot H₂O (B) {H₂L = 2-(hydroxyimino)-2-[(3-methoxyl-2-hydroxyphenyl)methylene]hydrazide, Hacac = acetylacetonone, $-\Delta S_m$ (A) = 31.23 J kg⁻¹ K⁻¹ for $\Delta H = 7$ T at 2 K, $-\Delta S_m$ (B) = 27.06 J kg⁻¹ K⁻¹ for $\Delta H = 7$ T at 2.5 K}; however, it is larger than some Gd₄ clusters: ^[25] [Gd₄(μ_3 -OH)₂L₆(acac)₄] \cdot 2CH₃CN {HL = 5-(4-o-hydroxybenzylidene)-8-hydroxylquinoline, acac = acetylacetonone, $-\Delta S_m = 18.85$ J kg⁻¹ K⁻¹ for $\Delta H = 7$ T at 2.5 K} and [Gd₄(dbm)₄(L)₆(μ_3 -OH)₂] \cdot 5CH₃CN ($-\Delta S_m = 16.35$ J K⁻¹ kg⁻¹ for $\Delta H = 7.0$ T at 3.0 K; HL = 5-(4-pyridinecarboxaldehyde)amino-8-hydroxylquinoline, dbm = 1,3-diphenyl-1,3-propanedione).

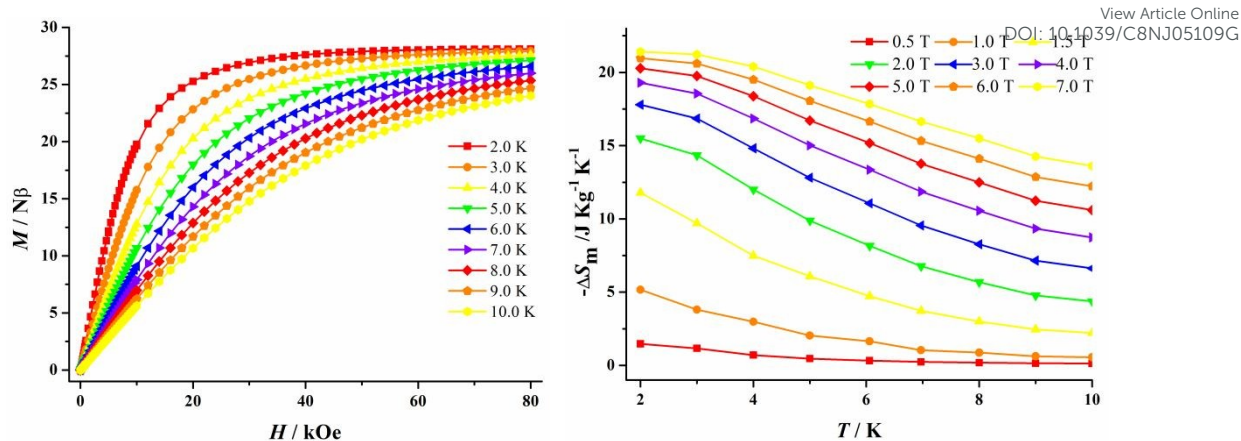


Figure 4. (Left) M versus H plots for **1** at $T = 2.0$ – 10.0 K and $H = 0$ – 80 kOe. (Right) Temperature dependence of magnetic entropy change ($-\Delta S_m$) as calculated from the magnetization data of **1** at $T = 2$ – 10.0 K and 0 – 7 T.

The variation of the magnetization with the applied magnetic field of **2** and **3** has been measured at 2 K in the field between 0 and 80 kOe, and shows a gradual increase of the magnetization at low fields. With the increasing of the field, **2** shows a saturation of 25 $N\beta$ at 80 kOe, while **3** exhibits a lack of saturation even at 80 kOe (Fig. S5). This behavior of **3** may be explained as the presence of magnetic anisotropy and/or the lack of a well defined ground state suggesting the presence of low-lying excited states that might be populated when a field is applied.^[26]

In order to investigate the dynamics of magnetization, the temperature dependences alternating current (AC) magnetic susceptibility measurements on **2** and **3** were performed in the temperature range 2–20 K and in the 111–2311 Hz frequency range with a 3 Oe ac magnetic field and under 0 dc field, however compound **2** (Tb_4) does not exhibit a frequency dependence under these conditions (Figure S6). As show in Figure 5, compound **3** displays clear frequency-dependence at low temperature, indicative of the possibility of SMM behaviour. Both the in-phase (χ') and out-of-phase (χ'') signals of **3** show an increasing trend in the low temperature zone, which may suggest the quantum tunneling of magnetization (QTM) were occurred in **3**. The difference of dynamics of magnetization between **2** and **3** may originate from the difference of intrinsic properties of lanthanide ions.

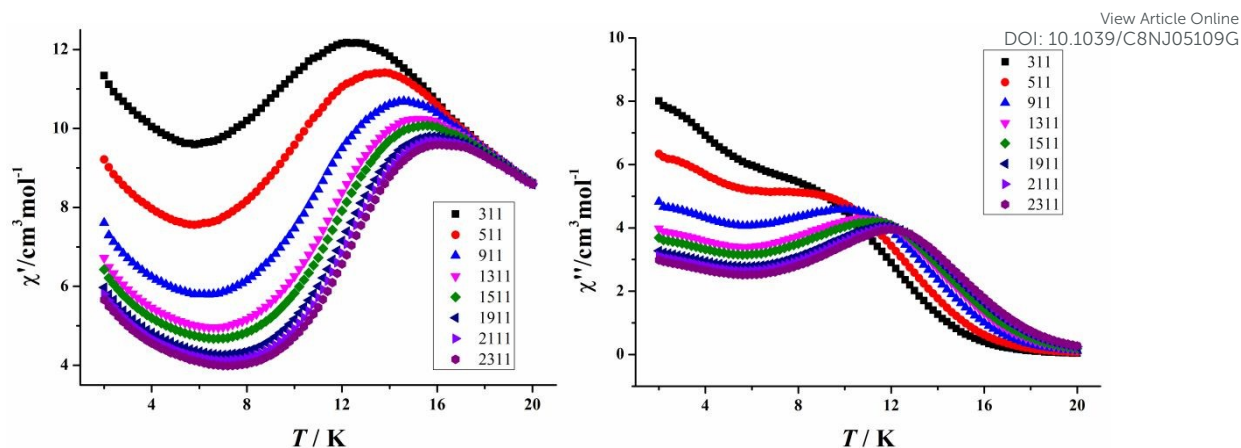


Figure 5. Temperature dependence of the in-phase (χ') and out-of-phase (χ'') ac susceptibilities for **3** in $H_{dc} = 0$ Oe with an oscillation of 3.0 Oe.

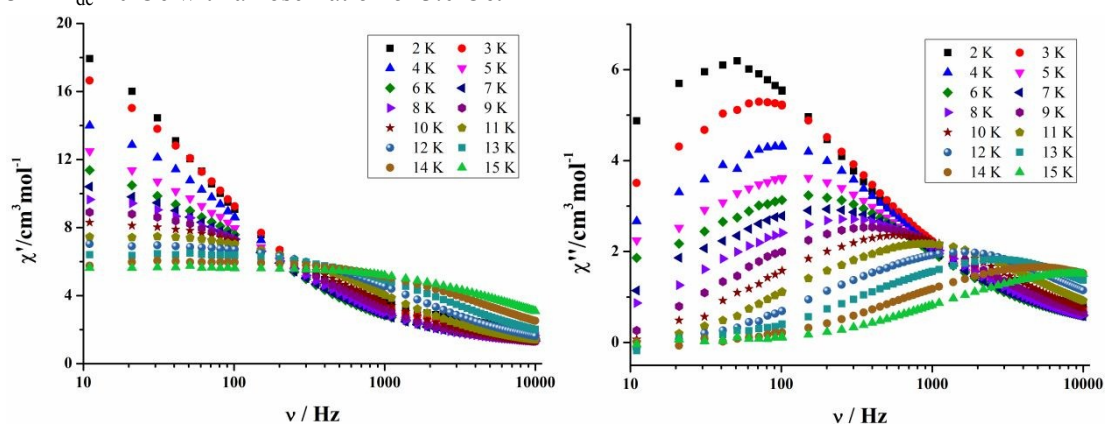


Figure 6. Frequency dependence of the in-phase (χ') and out-of-phase (χ'') ac susceptibilities for **3** at 2.0–16.0 K in $H_{dc} = 0$ Oe.

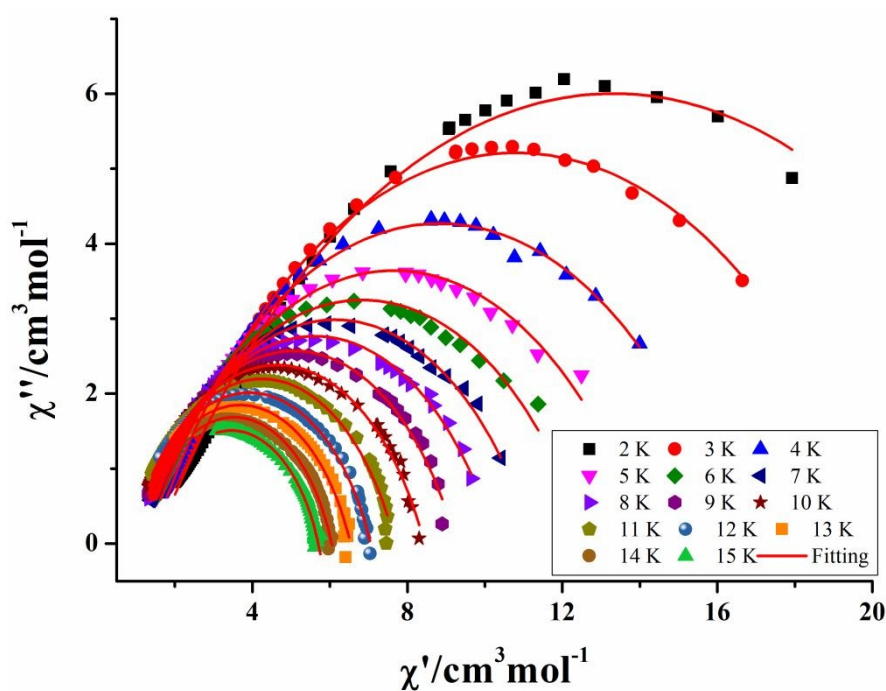


Figure 7. The cole-cole plot at different temperature in $H_{dc} = 0$ Oe.

In addition, to further understand the dynamics of magnetization of **3**, frequency dependence ac susceptibilities (Figure 6) were measured at 2-15 K under the zero dc fields, and the shape and frequency dependence further confirm the presence of single-molecule magnet behavior in **3**.^[27] The Cole - Cole plots of **3** are shown in Figure 7. A generalized Debye model was used in an attempt to fit the Cole-Cole diagram of **3** (Figure 7), and in the temperature range 2-15 K, α parameters are in the range of 0.25–0.40. The relatively small distribution coefficients α of the Dy₄ complexes indicate that there is a narrow distribution of relaxation time in **3**.^[28]

The relaxation time τ of **3** can be accessed from the frequency-dependent data, and the Arrhenius plot exhibit an obvious curvature (Figure 8), indicating that a combination of multiple relaxation pathways has to be taken into account. Data in the entire 3–14 K temperature range were analyzed by using the following equation:^[29]

$$\ln\tau = -\ln[AT + CT^n + \tau_0^{-1}\exp(-U_{\text{eff}}/k_{\text{B}}T)]$$

where AT , CT^n , and $\tau_0^{-1}\exp(U_{\text{eff}}/k_{\text{B}}T)$ represent direct, Raman, and Orbach relaxation processes, respectively. Least-squares fitting of $\ln\tau$ versus T^{-1} leads to $A = 19.42$, $n = 3.9$, $C = 0.03$, $U_{\text{eff}} = 81.48$ K, $\tau_0 = 6.48 \times 10^{-8}$ s and the agreement factor R , defined as $R = \sum(\chi_{\text{obsd}} - \chi_{\text{calcd}})^2 / \sum(\chi_{\text{obsd}})^2$, is 3.29×10^{-3} . The obtained pre-exponential factor (τ_0) is consistent with the reported values of 10^{-6} – 10^{-12} s for the Dy₄ clusters SMMs.^[30] The anisotropic energy barrier ($\Delta E/k_{\text{B}}$) of **3** is smaller than some reported Dy₄ compounds: $[\text{Dy}_4(\text{dbm})_4(\text{L})_6(\mu_3\text{-OH})_2] \cdot 4\text{CH}_3\text{CN} \cdot 2\text{H}_2\text{O}$ (L = 5-(4-pyridinecarboxaldehyde)amino-8-hydroxylquinoline, $U_{\text{eff}}/k_{\text{B}} = 89.38$ K),^[25b] $[\text{Dy}_4(\text{OH})_2(\text{bpt})_4(\text{NO}_3)_4(\text{OAc})_2]$ (Hbpt = 3,5-bis(pyridin-2-yl)-1,2,4-triazole, $U_{\text{eff}}/k_{\text{B}} = 206$ K),^[31] however, it is larger than some related tetranuclear dysprosium compounds in literature: $[\text{Ln}_4(\text{L})_2(\text{C}_6\text{H}_5\text{COO})_{12}(\text{MeOH})_4]$ (HL = 2,6-bis((furan-2-ylmethylimino)methyl)-4-methylphenol, $U_{\text{eff}}/k_{\text{B}} = 17.2$ K),^[32a] $[\text{Ln}_4(\mu_3\text{-OH})_2\text{L}_2(\text{acac})_6] \cdot 2(\text{CH}_3\text{CN})$ (L = N,N'-bis(salicylidene)-1,2-ethanediamine, acac = acetylacetonate, $U_{\text{eff}}/k_{\text{B}} = 13.95$ K),^[32b] $[\{(\text{LH})_2\text{Dy}_4\}(\mu_2\text{-O})_4](\text{H}_2\text{O})_8 \cdot 2\text{CH}_3\text{OH} \cdot 8\text{H}_2\text{O}$ (LH₃ = 6-hydroxymethyl)-N'-((8-hydroxyquinolin-2-yl)methylene)-picolinohydrazide, $U_{\text{eff}}/k_{\text{B}}$

= 54.2 K).^[32c]

View Article Online
DOI: 10.1039/C8NJ05109G

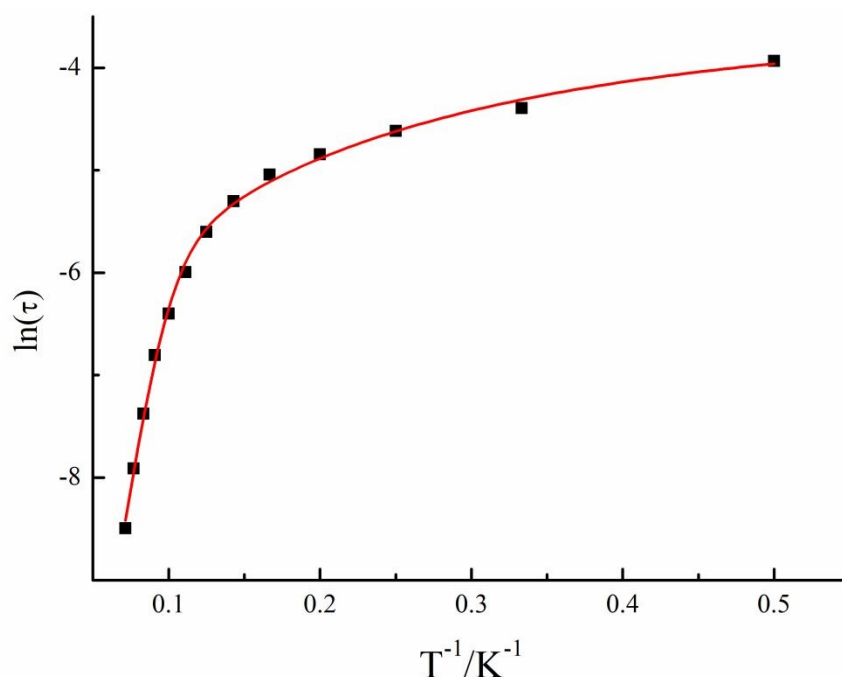


Figure 8. $\ln\tau$ versus T^{-1} plots for **3**. The red solid lines represent the least-squares fits of the experimental data to the Arrhenius law.

Conclusions

In summary, three tetranuclear lanthanide coordination complexes based on 5-(benzylideneamino)quinolin-8-ol have been constructed and structurally characterized. Systematic magnetic studies for them have been performed, **1** exhibits cryogenic magnetic refrigeration property with maximum $-\Delta S_m = 21.41 \text{ J K}^{-1} \text{ kg}^{-1}$ for a field change $\Delta H = 7 \text{ T}$ at 2.0 K); compound **3** exhibits slow relaxation of the magnetization with $U_{\text{eff}} = 81.48 \text{ K}$ and the preexponential factor $\tau_0 = 6.48 \times 10^{-8} \text{ s}$.

Acknowledgments

We gratefully acknowledge the National Natural Science Foundation of China (21501043, 21501079), the Natural Science Foundation of Education Department of Guizhou Province(KY[2015]454).

References

- [1] (a) D. N. Woodruff, R. E. P. Winpenny, R. A. Layfield, *Chem. Rev.*, 2013, **113**, 5110; (b) P.

- Zhang, Y. N. Guo, J. Tang, *Coord. Chem. Rev.*, 2013, **257**, 1728; (c) Y. Z. Zheng, Z. Zheng, X. M. Chen, *Coord. Chem. Rev.*, 2014, **258-259**, 1; (d) W.-M. Wang, S.-Y. Wang, H.-X. Zhang, H.-Y. Shen, J.-Y. Zou, H.-L. Gao, J.-Z. Cui, B. Zhao, *Inorg. Chem. Front.*, 2016, **3**, 133.
- [2] (a) X.-Y. Wang, C. Avendaño, K. R. Dunbar, *Chem. Soc. Rev.*, 2011, **40**, 3213; (b) S. J. Liu, J. P. Zhao, W. C. Song, S. D. Han, Z. Y. Liu, X. H. Bu, *Inorg. Chem.*, 2013, **52**, 2103; (c) Y. X. Chang, W. M. Wang, R. X. Zhang, H. Y. Shen, X. P. Zhou, N. N. Wang, J. Z. Cui, H. L. Gao, *New J. Chem.*, 2017, **41**, 6251; (d) X. L. Li, J. F. Wu, J. K. Tang, B. L. Guennic, W. Shi, P. Cheng, *Chem. Commun.*, 2016, **52**, 9570.
- [3] (a) Y.-Z. Zheng, G.-J. Zhou, Z. Zheng, R. E. P. Winpenny, *Chem. Soc. Rev.*, 2014, **43**, 1462; (b) S. J. Liu, C. Cao, C. C. Xie, T. F. Zheng, X. L. Tong, J. S. Liao, J. L. Chen, H. R. Wen, Z. Chang, X. H. Bu, *Dalton Trans.*, 2016, **45**, 9209; (c) S. J. Liu, C. Cao, S. L. Yao, T. F. Zheng, Z. X. Wang, C. Liu, J. S. Liao, J. L. Chen, Y. W. Li, H. R. Wen, *Dalton Trans.*, 2017, **46**, 64.
- [4] (a) S. K. Langley, B. Moubaraki, C. Tomasi, M. Evangelisti, E. K. Brechin, K. S. Murray, *Inorg. Chem.*, 2014, **53**, 13154; (b) X.-Y. Zheng, S.-Q. Wang, W. Tang, G.-L. Zhuang, X.-J. Kong, Y.-P. Ren, L.-S. Long, L.-S. Zheng, *Chem. Commun.*, 2015, **51**, 10687.
- [5] J. L. Liu, Y. C. Chen, F. S. Guo, M. L. Tong, *Coord. Chem. Rev.* 2014, **281**, 26.
- [6] (a) J.-B. Peng, X.-J. Kong, Q.-C. Zhang, M. Orendáč, J. Prokleška, Y.-P. Ren, L.-S. Long, Z.-P. Zheng, L.-S. Zheng, *J. Am. Chem. Soc.*, 2014, **136**, 17938; (b) Y.-Z. Zheng, M. Evangelisti, F. Tuna, R. E. P. Winpenny, *J. Am. Chem. Soc.*, 2012, **134**, 1057; (c) S. Das, A. Dey, S. Kundu, S. Biswas, R. S. Narayanan, S. Titos-Padilla, G. Lorusso, M. Evangelisti, E. Colacio, V. Chandrasekhar, *Chem. Eur. J.*, 2015, **21**, 16955; (d) K. Wang, Z. Chen, H.-H. Zou, k. Hu, H.-Y. Li, Z. Zhang, W.-Y. Sun, F. Liang, *Chem. Commun.*, 2016, **52**, 8297.
- [7] (a) Y. C. Chen, L. Qin, Z. S. Meng, D. F. Yang, C. Wu, Z. D. Fu, Y. Z. Zheng, J. L. Liu, R. Tarasenko, M. Orendáč, J. Prokleška, V. Sechovský, M. L. Tong, *J. Mater. Chem. A*, 2014, **2**, 985; (b) S. Biswas, H. S. Jena, A. Adhikary, S. Konar, *Inorg. Chem.*, 2014, **53**, 3926.
- [8] J. Dong, P. Cui, P. F. Shi, P. Cheng, B. Zhao, *J. Am. Chem. Soc.*, 2015, **137**, 15988.
- [9] Ishikawa, N.; Sugita, M.; Ishikawa, T.; Koshihara, S.-y.; Kaizu, Y., *J. Am. Chem. Soc.*, 2003, **125**, 8694.
- [10] (a) X. Jiang, C.M. Liu, H.-Z. Kou, *Inorg. Chem.*, 2016, **55**, 5880; (b) J. Xiong, H. Y. Ding, Y. S. Meng, C. Gao, X. J. Zhang, Z. S. Meng, Y. Q. Zhang, W. Shi, B. W. Wang, S. Gao, *Chem. Sci.*, 2017, **8**, 1288; (c) S. K. Gupta, T. Rajeshkumar, G. Rajaraman, R. Murugavel, *Chem. Sci.*, 2016, **7**, 5181; (d) S. Mukherjee, J. Lu, G. Velmurugan, S. Singh, G. Rajaraman, J. Tang, S. K. Ghosh, *Inorg. Chem.*, 2016, **55**, 11283; (e) S. Biswas, S. Das, S. Hossain, A. K. Bar, J.-P. Sutter, V. Chandrasekhar, *Eur. J. Inorg. Chem.* 2016, 4683.
- [11] (a) J. Liu, Y. C. Chen, J. L. Liu, V. Vieru, L. Ungur, J. H. Jia, L. F. Chibotaru, Y. Lan, W. Wernsdorfer, S. Gao, X. M. Chen, M. L. Tong, *J. Am. Chem. Soc.*, 2016, **138**, 5441; (b) W. M. Wang, X. M. Kang, H. Y. Shen, Z. L. Wu, H. L. Gao, J. Z. Cui, *Inorg. Chem. Front.*, 2018, **5**, 1876.
- [12] F.-S. Guo, B. M. Day, Y.-C. Chen, M.-L. Tong, A. Mansikkamäki, R. A. Layfield, *Angew. Chem. Int. Ed.*, 2017, **56**, 11445.
- [13] Y. S. Ding, N. F. Chilton, R. E. P. Winpenny, Y. Z. Zheng, *Angew. Chem., Int. Ed.*, 2016,

- 55, 16071.
- [14] P. Zhang, L. Zhang, C. Wang, S. F. Xue, S. Y. Lin, J. K. Tang, *J. Am. Chem. Soc.*, 2014, **136**, 4484.
- [15] L. F. Chibotaru, L. Ungur, A. Soncini, *Angew. Chem. Int. Ed.*, 2008, **47**, 4126.
- [16] (a) G. M. Sheldrick SHELXS-97, Program for the solution of crystal structure refinement. Germany: University of Göttingen, 1990; (b) G. M. Sheldrick SHELXTL-97, Program for X-ray crystal structure. Germany: University of Göttingen, 1997.
- [17] (a) M. Fang, P.-F. Shi, B. Zhao, D.-X. Jiang, P. Cheng, W. Shi, *Dalton Trans.*, 2012, **41**, 6820; (b) X. Y. Chu, H. X. Zhang, Y. X. Chang, Y. Y. Nie, J. Z. Cui, H. L. Gao, *New J. Chem.*, 2018, **42**, 5688; (c) Z.-L. Wu, Y.-G. Ran, X.-Y. Wu, Y.-P. Xia, M. Fang, W.-M. Wang, *Polyhedron*, 2017, **126**, 282.
- [18] (a) C. Benelli and D. Gatteschi, *Chem. Rev.*, 2002, **102**, 2369; (b) M. Fang, L.-J. Shao, T.-X. Shi, Y.-Y. Chen, H. Yu, P.-F. Li, W.-M. Wang, B. Zhao, *New J. Chem.*, 2018, **42**, 11847.
- [19] (a) M. Fang, H. Zhao, A. V. Prosvirin, D. Pinkowicz, B. Zhao, P. Cheng, W. Wernsdorfer, E. K. Brechin, K. R. Dunbar, *Dalton Trans.*, 2013, **42**, 14693; (b) W.-M. Wang, H.-H. Liu, L.-T. He, X.-R. Han, Z.-L. Wu, Y.-G. Ran, J.-Y. Zou, M. Fang, *Polyhedron*, 2017, **133**, 119.
- [20] (a) A. Panagiotopoulos, T. F. Zafiroopoulos, S. P. Perlepes, E. Bakalbassis, I. Masson-Ramade, O. Kahn, A. Terzis, C. P. Raptopoulou, *Inorg. Chem.*, 1995, **34**, 4918; (b) Z. H. Zhang, Y. Song, T. Okamura, Y. Hasegawa, W. Y. Sun, N. Ueyama, *Inorg. Chem.*, 2006, **45**, 2896.
- [21] O. Kahn. *Molecular Magnetism*, VCH Publisher, New York, 1993.
- [22] M. Evangelisti, A. Candini, A. Ghirri, M. Affronte, E. K. Brechin, E. J. L. McInnes, *Appl. Phys. Lett.*, 2005, **87**, 072504.
- [23] (a) L. X. Chang, G. Xiong, L. Wang, P. Cheng, B. Zhao, *Chem. Commun.*, 2013, **49**, 1055; (b) G. Xiong, H. Xu, J. Z. Cui, Q. L. Wang, B. Zhao, *Dalton Trans.*, 2014, **43**, 5639.
- [24] (a) J. A. Sheikh, A. Adhikary, S. Konar, *New J. Chem.*, 2014, **38**, 3006; (b) A. K. Mondal, H. S. Jena, A. Malviya, S. Konar, *Inorg. Chem.*, 2016, **55**, 5237; (c) W. M. Wang, Z. L. Wu, Y. X. Zhang, H. Y. Wei, H. L. Gao, J. Z. Cui, *Inorg. Chem. Front.*, 2018, **5**, 2346.
- [25] (a) W.-M. Wang, T.-L. Han, Y.-L. Shao, X.-Y. Qiao, Z.-L. Wu, Q.-L. Wang, P. F. Shi, H.-L. Gao, J.-Z. Cui, *New J. Chem.*, 2018, **42**, 14949; (b) H. L. Gao, S. X. Huang, X. P. Zhou, Z. Liu, J. Z. Cui, *Dalton Trans.*, 2018, **47**, 3503.
- [26] R. Pattacini, P. Teo, J. Zhang, Y. Lan, A. K. Powell, J. Nehr Korn, O. Waldmann, T. S. Andy Hor and P. Braunstein, *Dalton Trans.*, 2011, **40**, 10526.
- [27] (a) D. Gatteschi, R. Sessoli, J. Villain, *Molecular Nanomagnets*, Oxford University Press, Oxford, 2006; (b) S. D. Jiang, B. W. Wang, G. Su, Z. M. Wang, S. Gao, *Angew. Chem. Int. Ed.*, 2010, **49**, 7448.
- [28] Y.-N. Guo, G.-F. Xu, Y. Guo, J. Tang, *Dalton Trans.*, 2011, **40**, 9953.
- [29] (a) K. R. Meihaus, S. G. Minasian, W. W. Lukens, Jr., S. A. Kozimor, D. K. Shuh, T. Tyliczszak, J. R. Long, *J. Am. Chem. Soc.* 136 (2014) 6056; (b) J.-L. Liu, K. Yuan, J. D. Leng, L. Ungur, W. Wernsdorfer, F.-S. Guo, L. F. Chibotaru, M.-L. Tong, *Inorg. Chem.* 51 (2012) 8538; (c) X.-L. Li, H. Li, D.-M. Chen, C. Wang, J. Wu, J. Tang, W. Shi, P. Cheng, *Dalton Trans.* 44 (2015) 20316.
- [30] (a) W. Huang, F. X. Shen, S. Q. Wu, L. Liu, D. Y. Wu, Z. Zheng, J. Xu, M. Zhang, X. C.

- Huang, J. Jiang, F. F. Pan, Y. Li, K. Zhu, O. Sato, *Inorg. Chem.*, 2016, **55**, 5476; (b) M. J. Anwar, L. K. Thompson, L. N. Dawe, F. Habibb, M. Murugesu, *Chem. Commun.*, 2012, **48**, 4576.
- [31] P. H. Guo, J. Liu, Z. H. Wu, H. Yan, Y. C. Chen, J. H. Jia, M. L. Tong, *Inorg. Chem.*, 2015, **54**, 8087.
- [32] (a) S. Y. Lin, L. Zhao, H. Ke, Y. N. Guo, J. K. Tang, Yang Guo, J. M. Dou, *Dalton Trans.*, 2012, **41**, 3248; (b) W.-B. Sun, B.-L. Han, P.-H. Lin, H.-F. Li, P. Chen, Y.-M. Tian, M. Murugesu, P.-F. Yan, *Dalton Trans.*, 2013, **42**, 13397; (c) V. Chandrasekhar, S. Hossain, S. Das, S. Biswas, J.-P. Sutter, *Inorg. Chem.*, 2013, **52**, 6346.
- [33]

View Article Online
DOI: 10.1039/C8NJ05109G

1
2
3
4
5
6
7
8
9
10
11
12
13
14
15
16
17
18
19
20
21
22
23
24
25
26
27
28
29
30
31
32
33
34
35
36
37
38
39
40
41
42
43
44
45
46
47
48
49
50
51
52
53
54
55
56
57
58
59
60